

論文 / 著書情報  
Article / Book Information

Title	Damping Characteristics in Adaptation of Plastics for Robot Structures
Authors	Takeshi Takaki, Masahito Kanekiyo, Gen Endo
Citation	Proceedings of the 2023 IEEE/SICE International Symposium on System Integration, , ,
Pub. date	2023, 1
Copyright	(c) 2023 IEEE. Personal use of this material is permitted. Permission from IEEE must be obtained for all other uses, in any current or future media, including reprinting/republishing this material for advertising or promotional purposes, creating new collective works, for resale or redistribution to servers or lists, or reuse of any copyrighted component of this work in other works.
DOI	<a href="http://dx.doi.org/10.1109/SII55687.2023.10039233">http://dx.doi.org/10.1109/SII55687.2023.10039233</a>
Note	This file is author (final) version.

# Damping Characteristics in Adaptation of Plastics for Robot Structures

Takeshi Takaki<sup>1</sup>, Masahito Kanekiyo<sup>2</sup> and Gen Endo<sup>2</sup>

**Abstract**—Lightweighting is effective for high-speed operation in industrial robots. One method to achieve this is to use plastics, which are lighter than metallic materials, as structural materials. In addition, structural materials for industrial robots are required to have vibration damping properties. In this study, the damping properties of four types of aluminum alloy and seven types of plastic were investigated using a one-degree-of-freedom experimental machine as a simple model of an industrial robot. The damping ratio was observed to vary with amplitude. Therefore, we propose a variable damping ratio according to the amplitude. Experiments confirmed that this damping ratio can represent better actual phenomena than a constant damping ratio.

## I. INTRODUCTION

Lightweighting is effective in developing an industrial robot that can operate at high speeds. A method that actively uses plastics, which are lighter than metallic materials, is possible. In addition, for the accurate control of the end effector position, vibrations in the structural material must be damped quickly. The damping properties of aluminum alloys and plastics have been studied [1]-[4]. When plastic is used as a structural material, weight reduction can be expected, but its damping properties when used on an industrial robot are widely unknown. Therefore, it is necessary to evaluate the damping properties and to model the damping properties of structural materials to design a robot that can operate at high speeds. In this study, four types of aluminum alloy and seven types of plastic were used as test specimens to evaluate damping properties. Because the damping properties depend on the amplitude, we propose a variable damping ratio based on the amplitude. Experimental results show that actual phenomena can be better represented using the variable damping ratio.

## II. DAMPING RATIO

Let us consider the damping ratio  $\zeta$ . For simplicity, consider a system with an object of mass  $m$ , a damper of viscous resistance  $c$ , and a spring of stiffness  $k$ , as shown in Fig. 1. Let  $x$  and  $t$  be the amplitude and time, respectively. The equation of motion is given by

$$m \frac{d^2 x}{dt^2} + c \frac{dx}{dt} + kx = 0. \quad (1)$$

\*\*This research is subsidized by New Energy and Industrial Technology Development Organization (NEDO) under a project JPNP20016.

<sup>1</sup>Takeshi Takaki is with Graduate School of Advanced Science and Engineering, Hiroshima University, 1-4-1 Kagamiyama, Higashi-Hiroshima, Hiroshima, 739-8527 Japan, takaki@hiroshima-u.ac.jp

<sup>2</sup>Masahito Kanekiyo and Gen Endo are with the Department of Mechanical Engineering, Tokyo Institute of Technology, 2-12-1 Ookayama, Meguro-ku, Tokyo 152-8550, Japan, {kanekiyo.m.aa, endo.g.aa}@m.titech.ac.jp

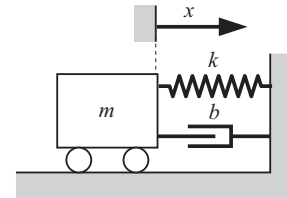


Fig. 1. Simplified model

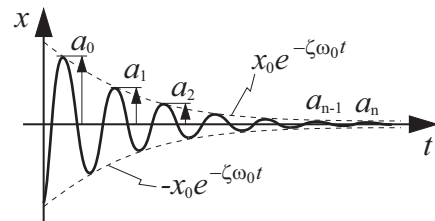


Fig. 2. Peak of damping vibration

If the system is damped and oscillating,  $x$  is solved as follows.

$$x = x_0 e^{-\zeta \omega_0 t} \sin(\omega_d t + \phi_0) \quad (2)$$

where  $x_0$  and  $\phi_0$  are values that depend on the initial values,  $\omega_0$  is the natural angular frequency, and  $\omega_d$  is the damped natural angular frequency.  $\omega_0$  and  $\omega_d$  have the following relationship.

$$\omega_d = \omega_0 \sqrt{1 - \zeta^2} \quad (3)$$

Let the peak of amplitude  $x$  be  $a_0, a_1, \dots, a_n$  as in Fig. 2. Here, the logarithms of the ratio of adjacent peaks are equal, and the following equation holds.

$$2\pi\zeta = \ln \frac{a_0}{a_1} = \ln \frac{a_1}{a_2} = \dots = \ln \frac{a_{n-1}}{a_n} \quad (4)$$

The damping ratio  $\zeta$  can be obtained using this equation. In Eq. (4),  $2\pi\zeta$  is obtained from one period, but let us consider obtaining it from  $n$  periods.  $2\pi\zeta n$  is given by

$$2\pi\zeta n = \ln \left( \frac{a_0}{a_1} \times \frac{a_1}{a_2} \times \dots \times \frac{a_{n-1}}{a_n} \right) = \ln \frac{a_0}{a_n}. \quad (5)$$

If Eq. (1) holds, the damping ratio  $\zeta$  is constant and independent of  $n$ . However, in the experiments described in Chapter III, the damping ratio  $\zeta$  obtained at different periods had different values; therefore, the damping ratio  $\zeta_n$  obtained from  $n$  periods is defined as in the following equation.

$$\zeta_n = \frac{1}{2\pi n} \ln \frac{a_0}{a_n} \quad (6)$$

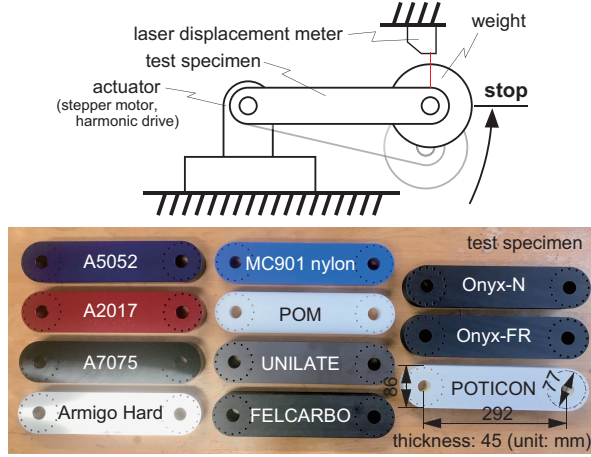


Fig. 3. Experimental setup

### III. EXPERIMENTS

#### A. Experimental setup

The aim of this experiment was to investigate the effect of changing the structural material of an industrial robot from aluminum alloy to plastic on the damping characteristics. As a simplified model of an industrial robot, we used the one-degree-of-freedom experimental setup shown in Fig. 3. Eleven different test specimens were tested. Four types of aluminum alloy (A2017, A5052, A7075, and Armigo Hard) and seven types of plastic (MC901 nylon, Onyx-FR, Onyx-N, POM, POTICON, FELCARBO, and UNILATE) were used. The Onyx-FR was fabricated using a Markforget 3D printer. The internal structure was fabricated Onyx with a filling rate of 37 % and reinforced with long carbon fibers on the top and bottom surfaces. Onyx-N was manufactured only with Onyx, and the internal structure was fabricated with a filling rate of 37 %. The sizes of the test specimens are shown in Fig. 3. An actuator was attached to one end of the test specimen, and a 3.2 kg weight was attached to the other end. The actuator (AZM98AC-HS100+AZD-A, Oriental motor co., Ltd.) was equipped with a closed-loop stepper motor, and the reduction gear was a harmonic drive. The amplitude  $x$  was measured using a laser displacement meter (LK-H150, LK-G5000, Keyence co.).

#### B. Experimental results

The experiment was conducted by lifting the weight until the test specimen was horizontal, stopping abruptly, and measuring the amplitude  $x$  of the resulting vibration. The experimental results are shown in Fig. 5. The damping ratios  $\zeta_1$ ,  $\zeta_3$ , and  $\zeta_{10}$  for each test specimen were obtained from 1, 3, and 10 cycles, as shown in Fig. 6.

Comparing the damping ratio  $\zeta$ , A2017 and Onyx-N had similar values. Here, a similar time response was expected to be obtained. However, as shown in Fig. 5, the experimental results showed that A2017 had a smaller amplitude  $x$  overall. Considering its use as a structural material for robots, A2017 is considered to be a superior material. In other words, when used for robotic applications, the time required for

TABLE I  
VARIABLE DAMPING RATIO PARAMETERS

Material	A	B
A2017	0.779	0.037
A5052	1.398	0.040
A7075	1.186	0.025
Armigo Hard	1.247	0.068
MC901 nylon	1.276	0.025
Onyx-FR	1.341	0.078
Onyx-N	0.323	0.061
POM	1.301	0.008
POTICON	1.211	0.020
FELCARBO	1.369	0.028
UNILATE	0.850	0.007

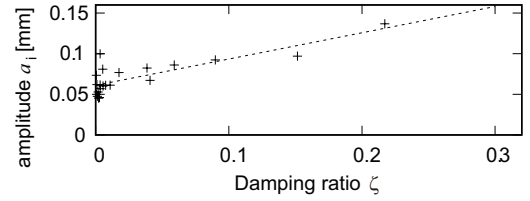


Fig. 4. Relationship between  $a_n$  and  $\zeta_n$  in Onyx-N

the amplitude  $x$  to become sufficiently small should be evaluated. Therefore, we defined the settling time  $t_s$  as the value at which the amplitude  $x$  becomes lower than the threshold value  $x_{th}$  at all times after that time, and we evaluated the results. The settling time  $t_s$  for each material with  $x_{th} = 0.01, 0.02$  and  $0.05$  mm is shown in Fig. 7.

#### C. Variable damping ratio

In the simple model described in Chapter 2, from Eq. (2),  $x$  oscillates between  $x = x_0 e^{-\zeta \omega_0 t}$  and  $x = -x_0 e^{-\zeta \omega_0 t}$ , as shown in Fig. 2. For reference,  $x = x_0 e^{-\zeta_i \omega_0 t}$  ( $i = 1, 3, 10$ ) is shown in Fig. 5 using  $\zeta_1$ ,  $\zeta_3$  and  $\zeta_{10}$  calculated from experiments in subsection III-B. The equation includes  $\omega_0$  and  $x_0$ . Let us consider  $\omega_0$ .  $\zeta_1$ ,  $\zeta_3$  and  $\zeta_{10}$  are sufficiently smaller than 1,  $\omega_0 \simeq \omega_d$  is assumed to hold from Eq. 3.  $\omega_d$  can be calculated using autocorrelation. Therefore,  $\omega_0$  can be obtained. The value of  $x_0$  is set to pass through the peak  $a_0$ . The settling times  $t_s$  when the damping ratio is  $\zeta_1$ ,  $\zeta_3$  and  $\zeta_{10}$  are shown in Fig. 7. When  $\zeta_1$  and  $\zeta_3$  are used for the damping ratio, the convergence is much faster than in the experiment, as shown in Fig. 7, indicating that the damped oscillations are not properly represented. In contrast,  $\zeta_{10}$  appears to be similar to the experimental value in Fig. 7, but the initial time response deviates significantly from the experimental value as shown in Fig. 5. In other words, the damping ratios  $\zeta_1$ ,  $\zeta_3$  and  $\zeta_{10}$  do not adequately represent the actual damped oscillations phenomena.

The damping ratio  $\zeta$  obtained from early periods tended to be larger. This indicates that the amplitude  $x$  is more heavily damped when the amplitude is large, and less damped as the amplitude is reduced. In other words,  $\zeta$  is considered to depend on  $x$ . For example, a plot of the amplitude peak  $a_i$  and the damping ratio  $\zeta_i$  for  $i = 1, 2, \dots, 21$  in Onyx-N is shown in Fig. 4. Therefore, we approximate this damping

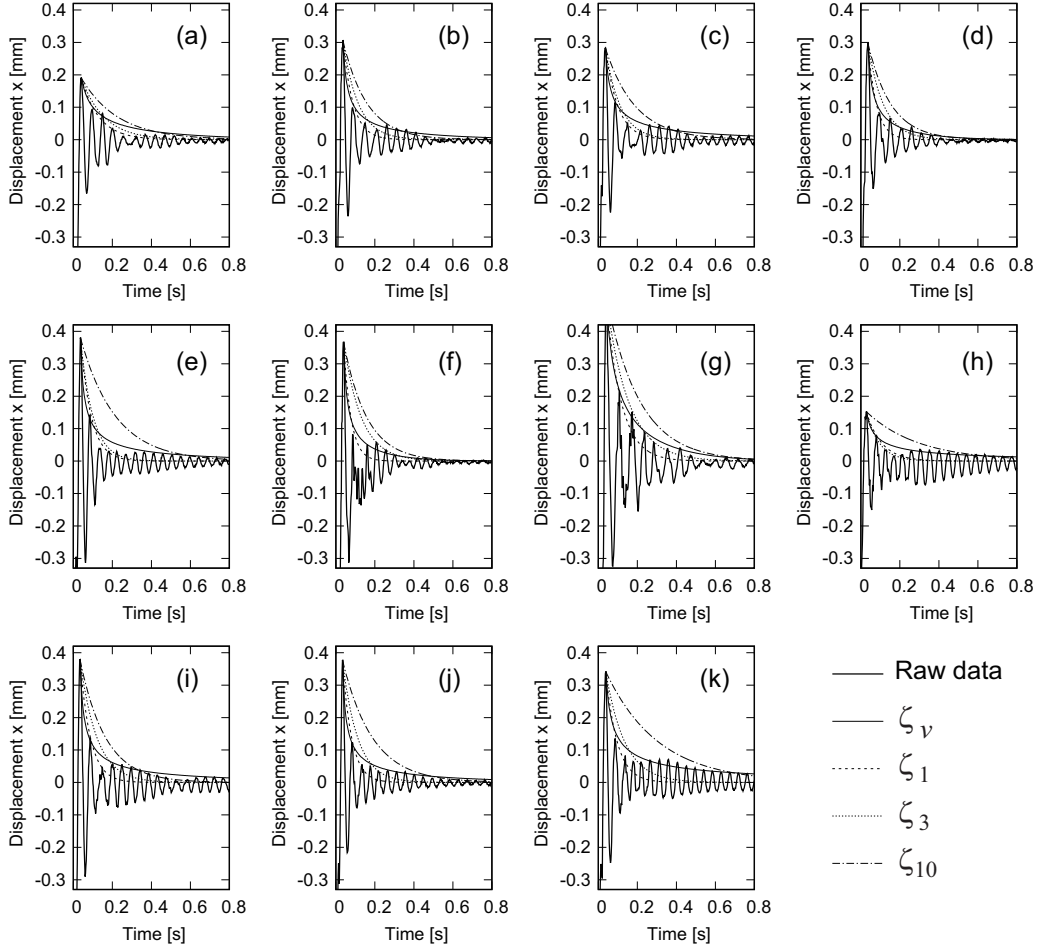


Fig. 5. Experimental results and damping ratio characteristics  $\zeta_1$ ,  $\zeta_3$  and  $\zeta_{10}$  a: A2017, b: A5052, c: A7075, d: Armigo Hard, e: MC901 nylon, f: Onyx-FR, g: Onyx-N, h: POM, i: POTICON, j: FELCARBO, k: UNILATE

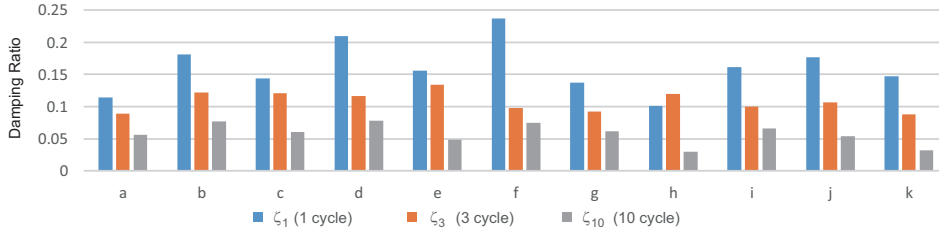


Fig. 6. Damping ratio  $\zeta_1$ ,  $\zeta_3$  and  $\zeta_{10}$  a: A2017, b: A5052, c: A7075, d: Armigo Hard, e: MC901 nylon, f: Onyx-FR, g: Onyx-N, h: POM, i: POTICON, j: FELCARBO, k: UNILATE

ratio as  $\zeta_v$  as a linear function of amplitude  $x$  as in the following equation.

$$\zeta_v = A|x| + B \quad (7)$$

where  $A$  and  $B$  are constants and are calculated using the least-squares method. The values of  $A$  and  $B$  calculated from  $a_i$  and  $\zeta_i$  when  $a_i$  is less than 0.025 mm are shown in Table I. Fig. 5 shows the time response when a variable damping ratio  $\zeta_v$  is used, and Fig. 7 shows the settling time. We can observe that both the time response and settling time were in good agreement compared with the case with a constant damping ratio.

#### D. Discussion

In the plastics, Onyx-FR was particularly superior in attenuation ratio  $\zeta$  and settling time  $t_s$ . Comparing only its numerical value, it was comparable to that of aluminum alloy. However, comparing the first peak  $a_0$ , the aluminum alloy was smaller. This was attributed to the higher rigidity of aluminum alloy. For most other plastics,  $a_0$  is considered to be larger than that of aluminum alloy for the same reason. In contrast, the damping properties of plastic are comparable to those of aluminum alloy, making it possible to use plastic as a structural material for robots in applications that do not require high rigidity.

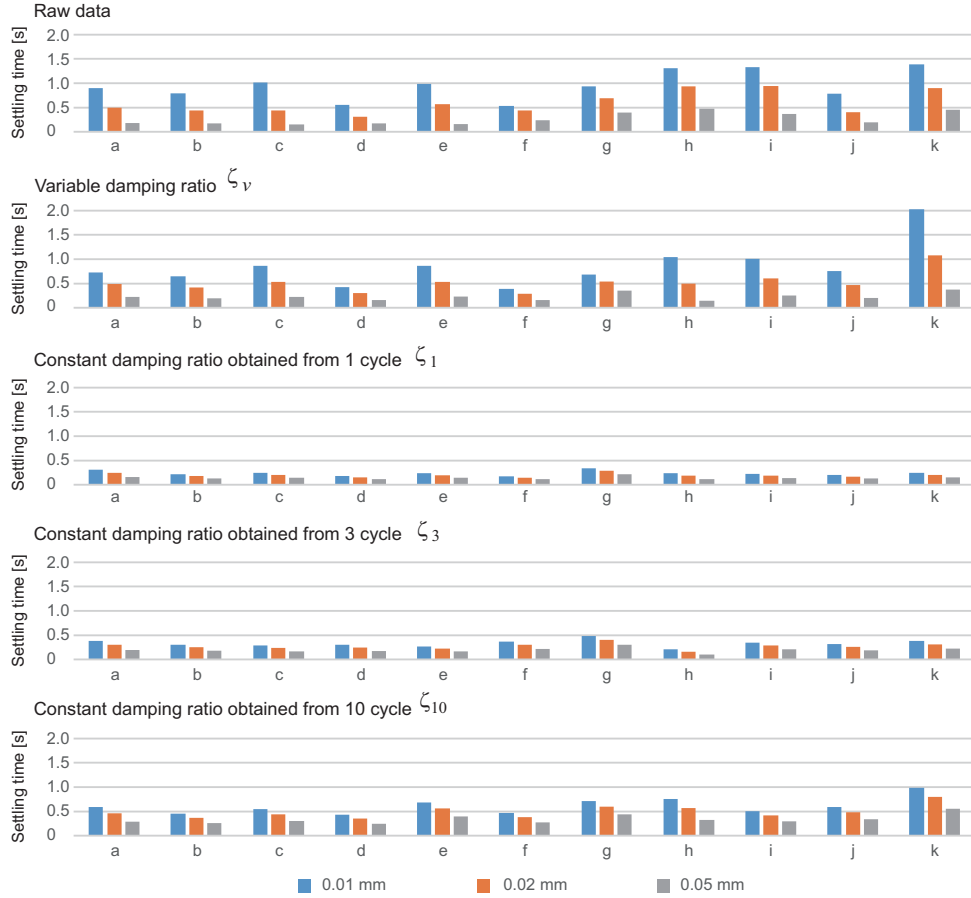


Fig. 7. Settling time, a: A2017, b: A5052, c: A7075, d: Armigo Hard, e: MC901 nylon, f: Onyx-FR, g: Onyx-N, h: POM, i: POTICON, j: FELCARBO, k: UNILATE

In this experiment, a phenomenon was observed in which the amplitude decreased once and increased again. This may be due to the influence of actuators, reduction gears, and its control system. In the future, the properties of structural materials should be examined separately from these characteristics. The variable damping ratio  $\zeta_v$  as a function of amplitude  $x$  was more consistent with the experimental data, suggesting that the damping characteristics depend on the amplitude  $x$ . In other words, it was necessary to verify the damping ratio  $\zeta$  for varying amplitude  $x$ . Considering the above, we plan to use a shaker to vibrate each element and clarify their characteristics.

#### IV. CONCLUSIONS

To investigate the possibility of replacing the robot's structural materials with plastic, we measured the damping properties of 11 different materials. Onyx reinforced with carbon fiber, for example, was observed to have damping properties comparable to those of aluminum alloy. However, the amplitude tended to be larger owing to the lower stiffness of the plastic. Additionally, we observed that the damping characteristics depend on the amplitude, and the proposed variable damping ratio can better represent actual phenomena. Because the damping ratio changes depending on the amplitude, we plan to use a shaker to vibrate the specimen

at various amplitudes to construct a more accurate model of the damping characteristics, which will be reflected in the robot design method.

#### ACKNOWLEDGMENT

This research is subsidized by New Energy and Industrial Technology Development Organization (NEDO) under a project JPNP20016. This paper is one of the achievements of joint research with and is jointly owned copyrighted material of ROBOT Industrial Basic Technology Collaborative Innovation Partnership.

We thank Prof. Yusuke Ohta (Chiba Institute of Technology), and Naoyuki Takesue (Tokyo Metropolitan University) for their valuable comments and discussion.

#### REFERENCES

- [1] X. Guan, H. Numakura, M. Koiwa: Internal Friction Peak in Cold-Worked "Pure" Aluminum and Aluminum Alloys, *J. de Physique IV Proceeding, EDF Sciences*, Vol. 6(C8), pp. 219-222, 1996.
- [2] T. C. Lei: Relationship between internal friction and creep rupture behavior of aluminum alloys, *J. de Physique Colloques*, Vol. 42(C5), pp. 487-492, 1981.
- [3] S. Dongli, Y. Dezhuang and Y. Zhengyao: Effect of heat treatment on internal friction of grain boundary in 2091 Al-Li alloy, *Trans. Nonferrous Met. Soc. China*, Vol. 7, No. 3, pp. 118-122, 1997.
- [4] T. Kawaguchi: Dynamic Mechanical Properties of Polyethylene Terephthalate, *J. Polymer science*, vol. 31. pp. 417-424, 1959.